VPS VIBRATIONS IN PHYSICAL SYSTEMS

DOI: 10.21008/j.0860-6897.2023.2.12
Vibrations in Physical Systems, 2023, 34(2), 2023212

The effect of sound-absorbing walls on the acoustic properties of the modelled unit cell of a sound-absorbing metamaterial

Aleksandra CHOJAK, Wojciech BINEK, Bartłomiej CHOJNACKI, Jan PAWLIK, Julia IDCZAK

AGH University of Krakow

Corresponding author: Aleksandra CHOJAK, email: achojak@agh.edu.pl

Abstract Cavity-based metamaterials are usually designed for sound absorbing or sound scattering properties. They are built of combinations of ducts and slits, which in the case of acoustic absorbers are designed to maximize the sound absorption at resonance frequencies through the appearance of the viscothermal losses. The unit cells are designed under the assumption of perfectly rigid walls, shared by all the analytical models. Sound absorbing properties of the structures result from viscothermal losses in small ducts. The paper discusses the influence of adding sound absorption to the walls in the numerical model on the results of the observed sound absorption coefficient. It is demonstrated that the resulting sound absorption of the structure varies with changing sound absorption coefficient of the walls of the structure. The same observations are made for 3D-printed measurement samples, showing the importance of including the sound absorption of the walls in the modelling process.

Keywords: sound absorption coefficient, FEM, metasurface.

1. Introduction

Acoustic metamaterials are engineered structures that present unusual properties, such as negative bulk modulus or negative mass density [1,2] which results in the desirable values of acoustic parameters, such as high sound absorption coefficient, sound diffusion, or transmission loss. The concept of metamaterials was translated into acoustics from electromagnetics in the 1990s – a photonic crystal was translated into a phononic crystal and presented frequency band gaps [3]. Since then, the development of acoustic metamaterials has begun and now different types of metamaterials are being investigated, such as membrane-type acoustic metamaterials [4], metamaterials with a periodic distribution of scatterers, i.e., phononic crystals [5], metamaterials with volumetric scatterers, such as Helmholtz resonators or quarter-wavelength resonators [6,7], or complex hybrid metamaterials [8]. The advantage of metamaterial structures over classic sound absorbers and diffusers, such as porous absorbers or QR diffusers is the reduction of their thickness. Due to the occurring sound dispersion, metamaterials work in a subwavelength frequency regime.

This paper concerns acoustic metamaterials with volumetric resonators, i.e. cavity-based metamaterials, working as sound absorbers. Analytical models, used for designing cavity-based metamaterials involve the plane wave expansion method (PWE), multiple scattering theory (MST), transfer matrix method (TMM), and finite element method modelling (FEM) [9]. All the analytical methods share the assumption that the walls of the designed unit cells are perfectly rigid and hence show no sound-absorbing properties (Neumann boundary condition), which is usually adopted in FEM models as well. This is generally true, when the walls are thick and heavy, compared to the wavelength of the resonance frequency of the structure. However, the idea behind designing metamaterials is to provide decreased dimensions of the structure compared to the effective wavelength. This is usually realized through loading the ducts with additional resonators placed in a transverse direction [6, 10, 11] or so-called coiling up space [7, 12–14] which involves the use of innovative manufacturing technologies such as 3D printing and may lead to arising sound absorption of the walls. Although it is not generally appointed as a problem, some authors acknowledge that the acoustic properties of the samples differ with different 3D printing technologies and also differ from the modelling results [15–17], usually increasing the value of the sound absorption coefficient. Little roughness caused by the layers, particularly in FDM-printed samples, results in a sound absorption coefficient which increases the resulting sound absorption of the unit cell. This paper discusses a particular case of a metamaterial, which is designed to be perfectly coupled and theoretically presents

a perfect absorption peak for the resonance frequency. The influence of additional sound absorption of the walls, which was not initially accounted for in the model, on the resulting sound absorption is discussed.

2. Model of the structure

The structure under study was similar to the one described in [7]. The geometry was changed in order to obtain the perfect absorption peak for ~550 Hz. The cross-section of the duct was changed into circular due to manufacturing reasons. The geometry of the sample and its dimensions are shown in Fig. 1 and in Tab. 1

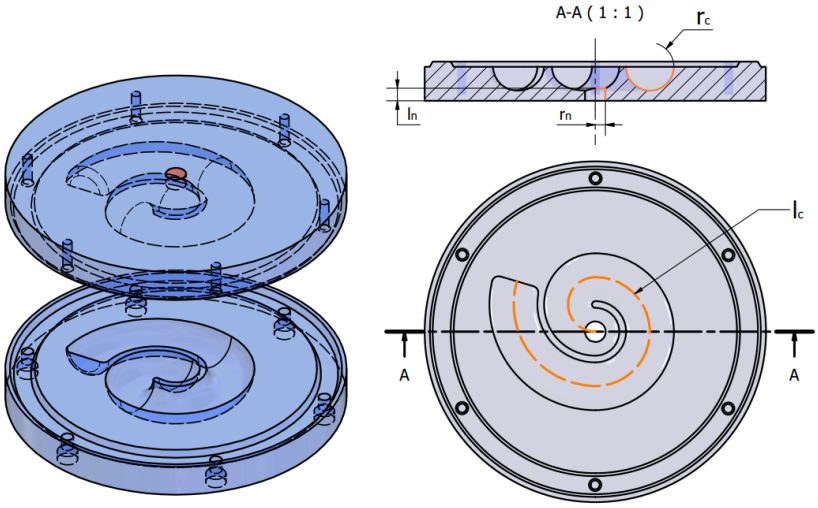

Figure 1. Scheme of the structure under study.

Table 1. Parameters of the structure under study

Area of the unit cell	Radius of the Neck, r_n	Length of the neck, l_n	Radius of the cavity, r_c	Length of the cavity, l_c
0.0079 m²	3 mm	3 mm	7 mm	120 mm

The structure was designed using Transfer Matrix Method (TMM) and verified with numerical simulations in COMSOL Multiphysics, using Finite Element Method (FEM). For the sake of TMM modelling, the geometry was simplified to a Helmholtz resonator with the neck and cavity dimensions as described by Tab. 1., by the rule of inverse coiling up space.

2.1. Transfer Matrix Method

The transfer Matrix Method (TMM) has been widely used in the literature to describe wave propagation in phononic crystals and acoustic metamaterialsc[6, 18]. It describes effectively sound dispersion and acoustic properties of the structures, such as reflection and transmission, leading to the typically used parameters, such as sound absorption coefficient, sound diffusion, scattering, and transmission loss. The transfer matrix method provides the relationship between the initial sound pressure $p(x)$ and acoustic velocity $v(x)$ at the face $(x = 0)$ and at the end $(x = L)$ of the modelled system. A transfer matrix takes the general form of:

$$\begin{bmatrix} p(x) \\ v(x) \end{bmatrix}_{x=0} = \mathbf{T} \begin{bmatrix} p(x) \\ v(x) \end{bmatrix}_{x=L} = \begin{bmatrix} T_{11} & T_{12} \\ T_{21} & T_{22} \end{bmatrix} \begin{bmatrix} p(x) \\ v(x) \end{bmatrix}_{x=L}. \tag{1}$$

In the case of a multi-layered system, e.g., a duct loaded with resonators, or a duct of varying cross-section, the matrix **T** is the product of the transfer matrixes for M subsequent layers:

$$\mathbf{T} = \prod_{m=1}^{M} \mathbf{T}^{(m)}. \tag{2}$$

The form of a single transfer matrix depends on the type of element and the connection between the elements. For a continuous fluid layer, such as a duct, slit, or a fluid layer, the transfer matrix takes the form of:

$$\mathbf{T}^{(m)} = \begin{bmatrix} \cos k_{\text{eff}} l_m & iZ_{\text{eff}} \sin k_{\text{eff}} l_m \\ i/_{Z_{\text{eff}}} \sin k_{\text{eff}} l_m & \cos k_{\text{eff}} l_m \end{bmatrix}, \tag{3}$$

where k_{eff} is the effective wave number in the layer, l_m is the length of the layer, and Z_{eff} is the effective characteristic impedance of the medium.

For a rigidly backed acoustic panel, which is the case for the discussed sample, sound reflection coefficient R can be derived from the transfer matrix as:

$$R = \frac{T_{11} - Z_0 T_{21}}{T_{11} + Z_0 T_{21}}, \tag{4}$$

where $Z_0 = \rho_0 c$ is the characteristic impedance of the surrounding medium (typically air), where ρ_0 is the air density and c – is the speed of sound. Sound absorption coefficient α is then defined as:

$$\alpha = 1 - |R|^2. \tag{5}$$

2.2. Effective parameters

For narrow ducts and slits, it is necessary to account for the viscothermal losses. It is done by evaluating complex and frequency-dependent density ρ_{eff} and bulk modulus κ_{eff} for each segment of the metamaterial structure. For a circular duct of radius r Stinson [19] gave the following formulas:

$$\rho_{\text{eff}} = \rho_0 \left[1 - \frac{2J_1(rG_\rho)}{rG_\rho J_0(rG_\rho)}\right], \tag{6}$$

$$\kappa_{\text{eff}} = \kappa_0 \left[1 + (\gamma - 1)\frac{2J_1(rG_\kappa)}{rG_\kappa J_0(rG_\kappa)}\right], \tag{7}$$

where ρ_0 is the equilibrium density of the medium, r is the radius of the duct, $\kappa_0 = \gamma P_0$, with $\gamma = 1.4$ being the heat capacity ratio, and P_0 static pressure, J_0 and J_1 are Bessel functions of the first kind and order 0 and 1, $G_\rho = \sqrt{-i\omega\rho_0/\eta}$, $G_\kappa = \sqrt{-i\omega \text{Pr}\rho_0/\eta}$, with Prandtl number $P_r = 0.71$, and dynamic viscosity of air $\eta = 1{,}813 \cdot 10^{-5} \frac{\text{kg}}{\text{ms}}$.

$$k_{\text{eff}} = \omega/\sqrt{\kappa_{\text{eff}}/\rho_{\text{eff}}}, \tag{8}$$

$$Z_{\text{eff}} = \frac{S_0}{S_a}\sqrt{\rho_{\text{eff}}\kappa_{\text{eff}}} \tag{9}$$

where $\omega = 2\pi f$ is the angular frequency, where f – frequency, S_0 is the area of the unit cell and S_a is the crossectional area of the duct.

In the case of the discussed structure, two length corrections must be included: Δl_1 resulting from the radiation from the neck to the free air, and Δl_2 resulting from a rapid change of the cross-section at the neck-cavity discontinuity. These can be accounted for as additional transfer matrixes for an in-line point element or simply by substituting l_m by l_{eff} in Eq. 3.

$$l_{\text{eff}} = l_n + \Delta l_1 + \Delta l_2, \tag{10}$$

where l_n is the length of the resonator neck. The correction Δl_1 is given by

$$\Delta l_1 = \frac{8r_n}{3\pi}, \tag{11}$$

where r_n is the radius of the resonator neck, and Δl_2 is given by:

$$\Delta l_2 = 0.822\left(1 - 1.33\frac{r_n}{r_c} + 0.17 * \left(\frac{r_n}{r_c}\right)^2 + 0.135 * \left(\frac{r_n}{r_c}\right)^3 + 0.29 * \left(\frac{r_n}{r_c}\right)^4\right), \tag{12}$$

where r_n is the radius of the resonator neck and r_n is the radius of the resonator cavity [20].

2.3. Numerical model

The most common approach to modelling metamaterials with finite element method is using *pressure acoustics* physics and modelling thermoviscous losses inside the ducts with effective parameters. In COMSOL Multiphysics this is realized by the *narrow region acoustics* branch. The model consisted of the air inside the modelled sample and a 10 cm high domain of air above the sample surface. Sound hard boundaries were applied to all the edges of the sample, as well as to the boundaries of the air domain above the sample in order to reflect the measurement conditions of an impedance tube. The acoustic field was generated by the background pressure field in the air above the sample, and the *plane wave radiation* condition was applied at the termination of the model to avoid sound reflection from the model boundary. In order to determine the sound absorption coefficient, the incident and reflected sound pressure were averaged over a plane 8 cm above the sample surface. The sound absorption coefficient was then determined by the use of Eq. 13

$$\alpha = 1 - \left|\frac{p_s}{p_b}\right|^2, \tag{13}$$

where p_s is the reflected sound pressure and p_b is the incident sound pressure.

The mesh was built of tetrahedral elements. The size of the elements was determined by the size of the ducts so that the mesh would reflect the actual geometry. The maximum element size was set to $\lambda/12$, λ being the wavelength for the highest frequency under study. The model is shown in Fig. 2.

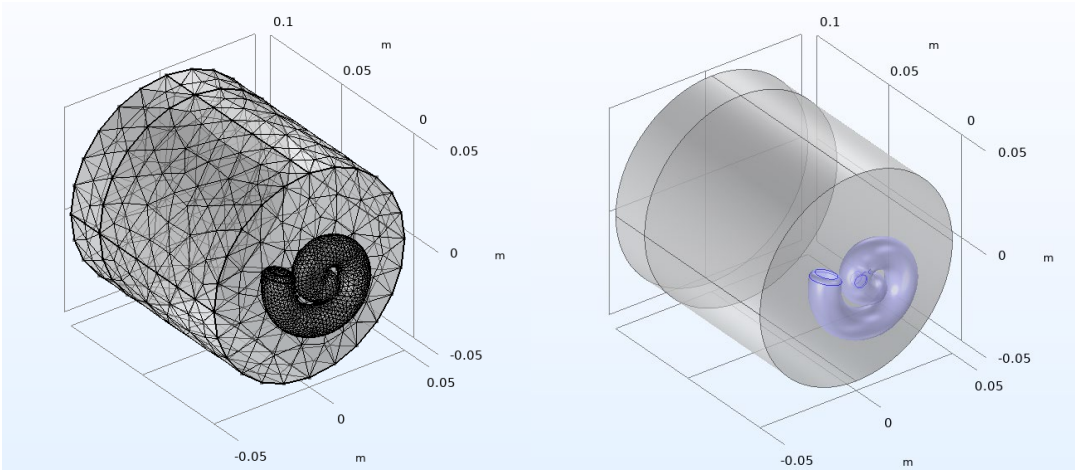

Figure 2. Finite element model of the structure under study: mesh (left) and domains with *narrow region acoustics* conditions applied (right).

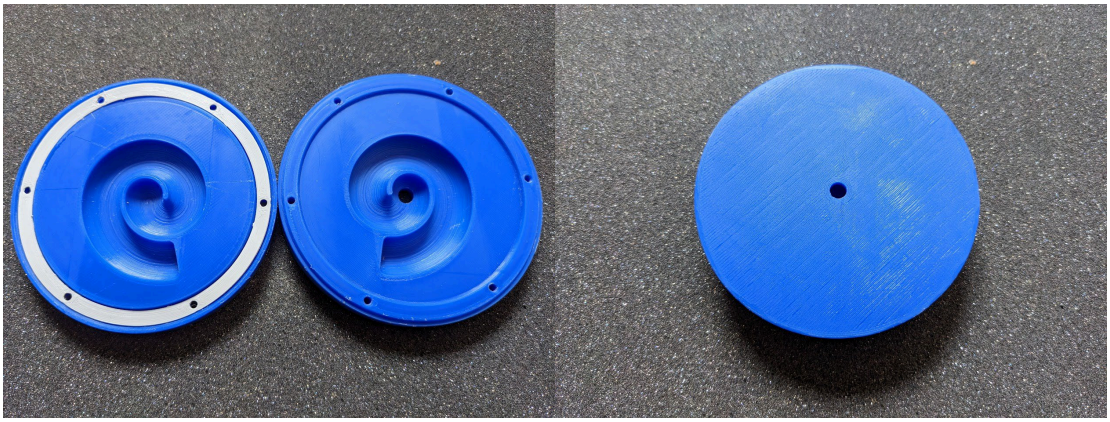

Figure 3. 3D printed sample of the structure under study.

2.4. Physical model

The structure was 3D printed with the use of FDM technology and PLA filament. The sample was printed in two halves, with a 3D printed TPU seal of minimal thickness, and six screws to ensure perfect sealing of the halves. The sample is shown in Fig. 3. The measurement of the sound absorption coefficient of the sample

was performed in an impedance tube, according to the transfer function method described in PN-EN ISO 10534-2 standard [21] in Bruel & Kjaer 4206 impedance tube.

2.5. Results and discussion

The results of the modelling and the measurements are shown in Fig. 4. For the modelling results (FEM and TMM) we can see a perfect agreement in terms of maximum sound absorption coefficient, which in both cases is equal to 0.99. The resonance frequency determined in the FEM model is 552 Hz and the one determined by TMM is 544 Hz. This difference results from the applied end correction – in a real-life scenario, the discontinuity is of a different geometry than the one assumed for the calculation of the end correction. However, the relative difference is less than 1.5%, which is a good agreement, despite the simplification of the modelled geometry.

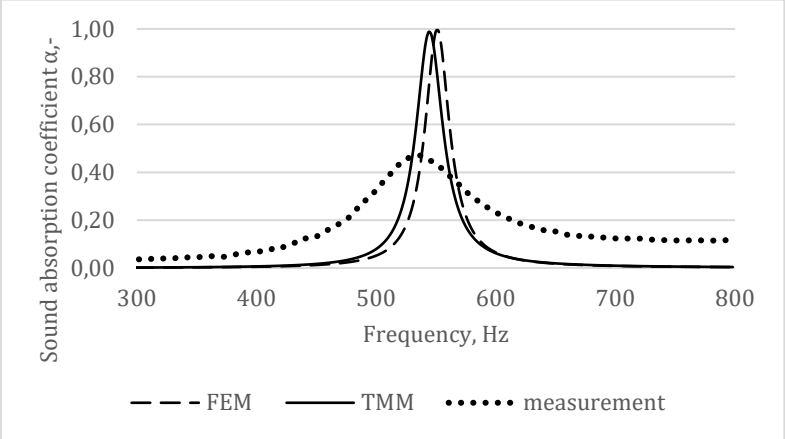

Figure 4. Sound absorption coefficient of the structure under study; modelling and measurement results.

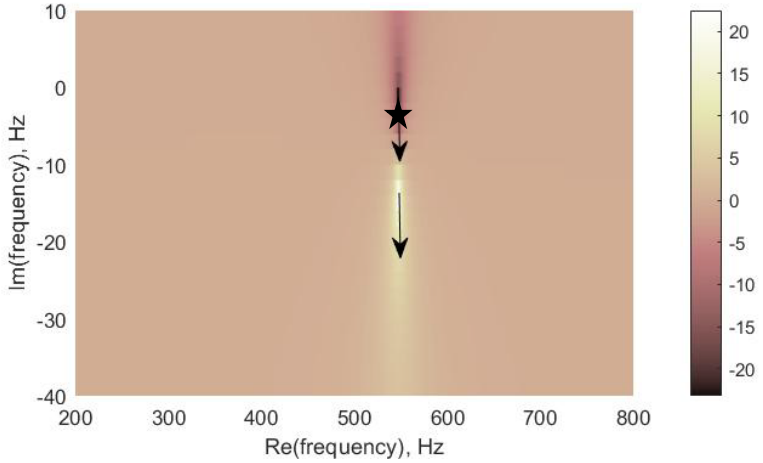

Figure 5. Common logarithm of the reflection coefficient of the modelled structure in a complex frequency plane. The star indicates the zero of the reflection coefficient, and the arrows show the direction of the change in the value of the reflection coefficient with increasing losses of the system.

However, the results of the measurement exhibit much lower values of the observed maximum sound absorption coefficient (0.47 vs 0.99). Since the 3D printed sample was perfectly sealed and the diameter of the sample provided tight fitting with the impedance tube, the differences can only be explained by the sound-absorbing properties of the walls, resulting from the roughness of the print.

The structure is designed to be perfectly coupled. It means that the radiation of the quasi-trapped mode from the Helmholtz resonator to the free air is balanced by the thermoviscous losses in the ducts forming the resonator. It is connected with the zero of the reflection coefficient observed for the real resonance frequency, with zero imaginary part [22] . Any additional absorption would cause a further shift of the zero-pole pair of the reflection coefficient in the complex frequency plane, resulting in lower absorption of the structure for the real part of the resonant frequency, i.e., the observed resonance frequency of the structure, which is what can be seen in the measurement results.

3. Model of the structure with sound-absorbing walls

In order to verify the impact of sound-absorbing walls on the resulting sound absorption coefficient of the structure, changes were made to the FEM model. The walls forming the resonator were prescribed with sound-absorbing properties. Since the walls of the print are only slightly rough, minimal values of sound absorption coefficients were prescribed: 0.01, 0.015, and 0.02 over the whole frequency range. The results of the modelling, compared to the results of the measurement, are set together in Fig. 6.

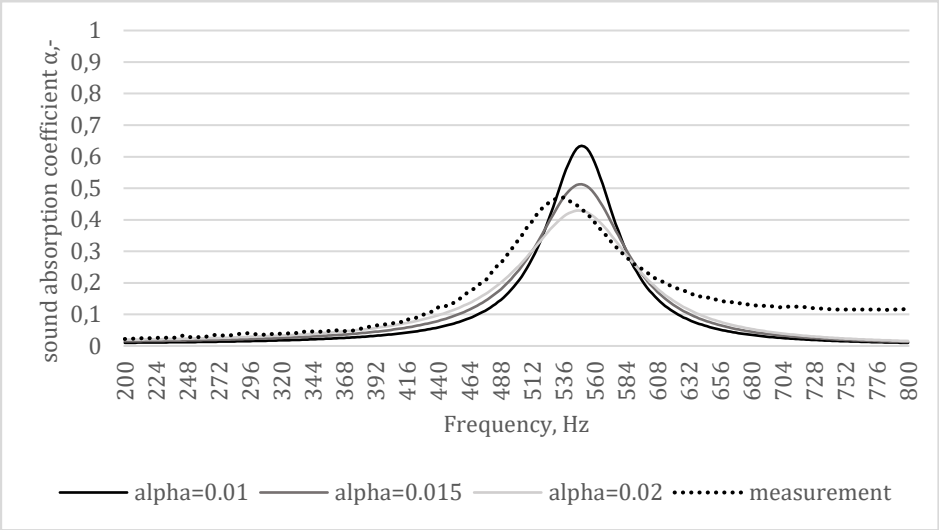

Figure 6. Sound absorption coefficient of the modelled structure with sound absorbing walls, numerical model.

Fig. 6 shows that introducing even minimal sound absorption to the walls of the structure makes a visible difference in the resulting sound absorption coefficient of the structure. The difference is observed mainly in the maximum of the sound absorption, which changes from 0.99 to 0.63, 0.51, and 0.43 for the increasing values of the sound absorption coefficient of the structure walls. What is also important, the Q-factor of the absorption curve increases and matches the measurement results better. Correspondingly, the values of the fractional bandwidths, defined as the ratio of the bandwidth to the resonance frequency of the structure change from 3,99% for the case with perfectly reflecting walls to 12.36%, 16%, and 19.71% for increasing values of the sound absorption coefficient of the structure walls. For comparison, the fractional bandwidth of the measured absorption curve is 21.64%. Together with the maximum value of 0.47, it corresponds best to the case of 0.02 of sound absorption of the walls.

In order to verify the above conclusions, a modified version of the structure was proposed. The ducts were broadened in order to decrease the viscothermal losses and compensate them with sound absorption of the walls. The geometry of the new structure is shown in Tab. 2. The structure was also 3D-printed; the parameters of the print, as well as the filament and the construction details, remained unchanged in comparison with the initial design. The only difference was in the geometrical dimensions of the structure.

Table 2. Parameters of the structure after modification.

Area of the unit cell	Radius of the Neck, r_n	Length of the neck, l_n	Radius of the cavity, r_c	Length of the cavity, l_c
0.0079 m²	4 mm	2 mm	10 mm	120 mm

The results of the modelling and the measurement of the new structure are shown in Fig. 7. We can see a very good agreement of the sound absorption curves. The resonance frequency of the measured and the modelled sample overlap. The maximum value obtained in the measurement is 0.78 and 0.79 in the

numerical model. The values of the fractional bandwidths are 20.6% and 17.6% for the measurement and numerical results, respectively.

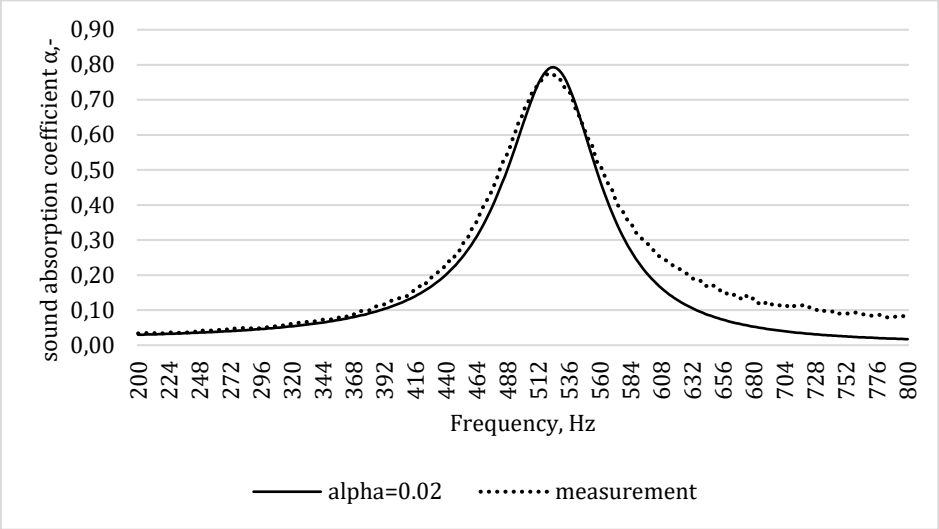

Figure 7. Sound absorption coefficient of the structure with modified geometry, modelled with sound absorbing walls, and measured.

4. Conclusions

Cavity-based sound-absorbing metamaterials are normally designed under the assumption that the walls of the structure are perfectly rigid and hence show now sound absorbing properties and the absorbing properties of the structures are achieved due to other phenomena, such as thermoviscous losses in the ducts. In real applications, this assumption is hardly possible to be achieved. Even small imperfections of the surface may result in minimal values of the sound absorption coefficient. In the paper, the effects of such minimal imperfections on the resulting sound absorption coefficient of a metamaterial unit cell were discussed. The unit cell under study was built of a Helmholtz resonator with a spiral cavity. A numerical model of such a metamaterial was discussed and compared with the analytical model derived with the use of the transfer matrix method. A good agreement between the models was achieved. Then, the sound absorption coefficient of a 3D printed sample was measured in an impedance tube and a large difference between the results of the modelling and the measurement results was observed. The difference was explained by excess losses which caused a shift of the zero of the reflection coefficient in the complex frequency plane. In order to verify that the difference between the measurement and numerical results was caused by the absorption of the walls, in the next step, minimal values of sound absorption coefficient were applied to the walls in the numerical model in order to match the results of the measurement. In the end, a structure with a modified geometry was proposed. The radii of the cross-sections were increased to balance the additional sound absorption with the reduced viscothermal losses. A very good agreement was obtained between the results of the numerical simulations and the measurement results.

Additional information

The project was funded and supported by the Polish Government, National Centre of Research and Development, agreement no. LIDER/11/0065/L-12/20/NCBR/2021.

The author(s) declare: no competing financial interests and that all material taken from other sources (including their own published works) is clearly cited and that appropriate permits are obtained.

References

1. Y. Ding, Z. Liu, C. Qiu, J. Shi. Metamaterial with simultaneously negative bulk modulus and mass density. Phys Rev Lett 99 (3)9, 2007, 93904,
2. J.-P. Groby, W. Huang, A. Lardeau, Y. Aurégan. The use of slow waves to design simple sound absorbing materials. J Appl Phys 117 (3)12, 2015, 124903,
3. M.M. Sigalas, E.N. Economou. Elastic and acoustic wave band structure. J Sound Vib 158 (3)2, 1992, 377–82,

4. G. Ma, M. Yang, S. Xiao, Z. Yang, P. Sheng. Acoustic metasurface with hybrid resonances. Nat Mater 13 (3)9, 2014, 873–8,
5. M.S. Kushwaha, P. Halevi, L. Dobrzynski, B. Djafari-Rouhani. Acoustic band structure of periodic elastic composites. Phys Rev Lett 71 (3)13, 1993, 2022,
6. N. Jiménez, V. Romero-García, V. Pagneux, J.P. Groby. Rainbow-trapping absorbers: Broadband, perfect and asymmetric sound absorption by subwavelength panels for transmission problems. Sci Rep 7 (3)1, 2017, 1–13,
7. S. Huang, X. Fang, X. Wang, B. Assouar, Q. Cheng, Y. Li. Acoustic perfect absorbers via spiral metasurfaces with embedded apertures. Appl Phys Lett 113 (3)23, 2018, 233501,
8. Y. Tang, S. Ren, H. Meng, F. Xin, L. Huang, T. Chen, et al. Hybrid acoustic metamaterial as super absorber for broadband low-frequency sound. Sci Rep 7 (3)February, 2017, 1–11,
9. N. Jiménez, J.P. Groby, V. Romero-García. Acoustic waves in periodic structures, metamaterials, and porous media. Ch. the Transfer Matrix Method in Acoustics, Springer International Publishing, Cham 2021, 103–64,
10. N. Jiménez, W. Huang, V. Romero-García, V. Pagneux, J.-P. Groby. Ultra-thin metamaterial for perfect and quasi-omnidirectional sound absorption. Appl Phys Lett 109 (3)12, 2016, 121902,
11. V. Romero-García, G. Theocharis, O. Richoux, A. Merkel, V. Tournat, V. Pagneux. Perfect and broadband acoustic absorption by critically coupled sub-wavelength resonators. Sci Rep 6 (3)1, 2016, 1–8,
12. Z. Liang, J. Li. Extreme acoustic metamaterial by coiling up space. Phys Rev Lett 108 (3)11, 2012, 114301,
13. X. Ni, Y. Wu, Z.-G. Chen, L.-Y. Zheng, Y.-L. Xu, P. Nayar, et al. Acoustic rainbow trapping by coiling up space. Sci Rep 4 (3)1, 2014, 7038,
14. T. Cambonie, F. Mbailassem, E. Gourdon. Bending a quarter wavelength resonator: Curvature effects on sound absorption properties. Applied Acoustics 1312018, 87–102,
15. A. Ciochon, J. Kennedy, M. Culleton. Evaluation of surface roughness effects on additively manufactured acoustic materials.
16. T.G. Zieliński, K.C. Opiela, P. Pawłowski, N. Dauchez, T. Boutin, J. Kennedy, et al. Reproducibility of sound-absorbing periodic porous materials using additive manufacturing technologies: Round robin study. Addit Manuf 362020, 101564,
17. T.G. Zieliński, N. Dauchez, T. Boutin, M. Leturia, A. Wilkinson, F. Chevillotte, et al. Taking advantage of a 3D printing imperfection in the development of sound-absorbing materials. Applied Acoustics 1972022, 108941,
18. A. Dell, A. Krynkin, K. V Horoshenkov. The use of the transfer matrix method to predict the effective fluid properties of acoustical systems. Applied Acoustics 1822021, 108259,
19. M.R. Stinson. The propagation of plane sound waves in narrow and wide circular tubes, and generalization to uniform tubes of arbitrary cross-sectional shape. J Acoust Soc Am 89 (3)2, 1991, 550–8,
20. A.I. Komkin, A.I. Bykov. Inertial attached neck length of Helmholtz resonators. Acoust Phys 622016, 269–79,
21. EN ISO 10534-2. Determination of sound absorption coefficient and impedance in impedance tubes, Part 2: Transfer-function method. 2003.
22. V. Romero-García, G. Theocharis, O. Richoux, V. Pagneux. Use of complex frequency plane to design broadband and sub-wavelength absorbers. J Acoust Soc Am 139 (3)6, 2016, 3395–403,